

Transdimensional Tunneling in the Multiverse

Jose J. Blanco-Pillado, Delia Schwartz-Perlov, and Alexander Vilenkin

Institute of Cosmology, Department of Physics and Astronomy,

Tufts University, Medford, MA 02155, USA

Abstract

Topology-changing transitions between vacua of different effective dimensionality are studied in the context of a 6-dimensional Einstein-Maxwell theory. The landscape of this theory includes a 6d de Sitter vacuum (dS_6), a number of $dS_4 \times S_2$ and $AdS_4 \times S_2$ vacua, and a number of $AdS_2 \times S_4$ vacua. We find that compactification transitions $dS_6 \rightarrow AdS_2 \times S_4$ occur through the nucleation of electrically charged black hole pairs, and transitions from dS_6 to $dS_4 \times S_2$ and $AdS_4 \times S_2$ occur through the nucleation of magnetically charged spherical black branes. We identify the appropriate instantons and describe the spacetime structure resulting from brane nucleation.

I. INTRODUCTION

String theory, as well as other higher-dimensional theories, suggests the existence of a landscape of vacua with diverse properties. The vacua are characterized by different compactifications of extra dimensions, by branes wrapped around extra dimensions in different ways, by different values of fluxes, etc. The number of possibilities is combinatorial and can be as high as 10^{1000} [1]. In the cosmological context, high-energy vacua drive exponential inflationary expansion of the universe. Transitions between different vacua occur through tunneling [2] and quantum diffusion [3, 4], with regions of different vacua nucleating and expanding in the never-ending process of eternal inflation. As a result, the entire landscape of vacua is explored. This “multiverse” picture has been a subject of much recent research.

Most of this recent work has focused on the sector of the landscape with 3 large spatial dimensions and the rest of the dimensions compactified. If all vacua had this property, we would be able to describe the entire multiverse by a 4-dimensional effective theory. However, the landscape generally includes states with different numbers of compactified dimensions. Even a simple toy model based on a 6-dimensional Einstein-Maxwell theory exhibits vacua with 0, 2, and 4 compact dimensions. We therefore expect the multiverse to include regions of different (effective) dimensionality [5].

Topology-changing transitions between vacua with different numbers of compact dimensions have been discussed in Refs. [5–8] in the context of Einstein-Maxwell theory compactified on a sphere. The radius of the compact dimensions in this theory is stabilized by a magnetic flux through the sphere, but the resulting vacua are only metastable and can decay by quantum tunneling through a barrier.¹ The tunneling results in the formation of an expanding bubble, inside of which the compact sphere is destabilized and its radius grows with time. Transitions of this sort are called *decompactification* transitions. The *compactification* tunneling transitions go in the opposite direction: the number of compact dimensions increases from parent to daughter vacuum. Such transitions have been discussed in the interesting recent paper by Carroll, Johnson and Randall [8], who also obtained an estimate of the transition rate. Our main goal in the present paper is to elucidate the nature of the tunneling instantons and the spacetime geometry resulting from topology-changing

¹ The model of Ref. [5] had an extra ingredient – the inflaton field – and a different mechanism of decompactification. The inflaton undergoes quantum diffusion in the course of eternal inflation, and the compact dimensions are destabilized whenever the inflaton potential gets below certain critical values.

transitions.

In the next Section we begin with a brief review of flux vacua in the $6d$ Einstein-Maxwell theory. Compactification tunneling transitions from $6d$ to effectively $2d$ and $4d$ spacetimes are discussed in Sections III and IV, respectively, and decompactification transitions are discussed in Section V. Our conclusions are summarized and discussed in Section VI.

II. THE LANDSCAPE OF $6d$ EINSTEIN-MAXWELL THEORY

We shall consider a 6-dimensional Einstein-Maxwell theory,

$$S = \int d^6x \sqrt{-\tilde{g}} \left(\frac{1}{2} \tilde{R}^{(6)} - \frac{1}{4} F_{MN} F^{MN} - \Lambda_6 \right), \quad (1)$$

where $M, N = 0 \dots 5$ label the six-dimensional coordinates, F_{MN} is the Maxwell field strength, Λ_6 is the six-dimensional cosmological constant, $\tilde{R}^{(6)}$ is the 6-dimensional curvature scalar, and we use units in which the $6d$ Planck mass is $M_6 = 1$. We shall assume that $\Lambda_6 > 0$. This model has a long pedigree [9, 10]; more recently it has been discussed as a toy model for string theory compactification [11].

Flux vacua are described by solutions of this model with the spacetime metric given by a $(6 - q)$ -dimensional maximally symmetric space of constant curvature and a static q -dimensional sphere of fixed radius, namely a metric of the form,

$$ds^2 = \tilde{g}_{MN} dx^M dx^N = \tilde{g}_{\mu\nu} dx^\mu dx^\nu + R^2 d\Omega_q^2. \quad (2)$$

Here, $\tilde{g}_{\mu\nu}$ is the metric of the $(6 - q)$ -dimensional de Sitter, Minkowski, or anti-de Sitter space, and $d\Omega_q^2$ is the metric on a unit q -sphere. We shall use the convention that the Greek indices label the large dimensions and take values $\mu, \nu = 0, 1, \dots, 5 - q$. The compact dimensions will be labeled by indices from the beginning of the Latin alphabet, $a, b = 6 - q, \dots, 5$.

The simplest solution of the model, corresponding to $q = 0$, is the $6d$ de Sitter space with $F_{MN} = 0$.

For $q = 2$, the only ansatz for the Maxwell field that is consistent with the symmetries of the metric is a monopole-like configuration on the extra-dimensional 2-sphere [10],

$$F_{ab} = \frac{Q_m}{4\pi} \sqrt{g_2} \epsilon_{ab}, \quad (3)$$

where Q_m is the corresponding magnetic charge and g_2 is the determinant of the metric on a unit 2-sphere. All other components of F_{MN} are equal to zero. We shall assume that

our model includes electrically charged particles with elementary charge e (not shown in the action (1)). Then the magnetic charge is subject to the usual charge quantization condition,

$$Q_m = \frac{2\pi n}{e}, \quad (4)$$

where n is an integer. This sector of the model can be described in terms of an effective $4d$ field theory. Representing the $6d$ metric as

$$ds^2 = e^{-\psi(x)/M_4} g_{\mu\nu} dx^\mu dx^\nu + e^{\psi(x)/M_4} R^2 d\Omega_2^2 \quad (5)$$

and integrating over the internal manifold, we obtain

$$S = \int d^4x \sqrt{-g} \left(\frac{1}{2} M_4^2 R^{(4)} - \frac{1}{2} \partial_\mu \psi \partial^\mu \psi - V(\psi) \right). \quad (6)$$

Here, the potential for the size of the internal dimension is

$$V(\psi) = 4\pi \left(\frac{n^2}{8e^2 R^2} e^{-3\psi/M_4} - e^{-2\psi/M_4} + R^2 \Lambda_6 e^{-\psi/M_4} \right) \quad (7)$$

and

$$M_4^2 = 4\pi R^2, \quad (8)$$

is the $4d$ Planck mass.

For any particular value of n , we can set the minimum of the potential to be at $\psi = 0$, by setting

$$R^2 = \frac{1}{\Lambda_6} \left(1 - \sqrt{1 - \frac{3n^2 \Lambda_6}{8e^2}} \right). \quad (9)$$

The $4d$ cosmological constant is the value of the potential at this minimum and is given by

$$\Lambda_4 = V(\psi = 0, n) = \frac{4\pi}{3} \left(1 - 2\sqrt{1 - \frac{3n^2 \Lambda_6}{8e^2}} \right). \quad (10)$$

Positive-energy vacua are obtained for

$$n > n_0 \equiv \left(\frac{2}{\Lambda_6} \right)^{1/2} e. \quad (11)$$

The potential also has a maximum at some $\psi > 0$ and approaches zero at $\psi \rightarrow \infty$, as illustrated in Fig. 1. It is clear from the figure that a positive-energy vacuum can decay by tunneling through a barrier, leading to decompactification of extra dimensions².

² Perturbative stability in similar models has been discussed in [12, 13].

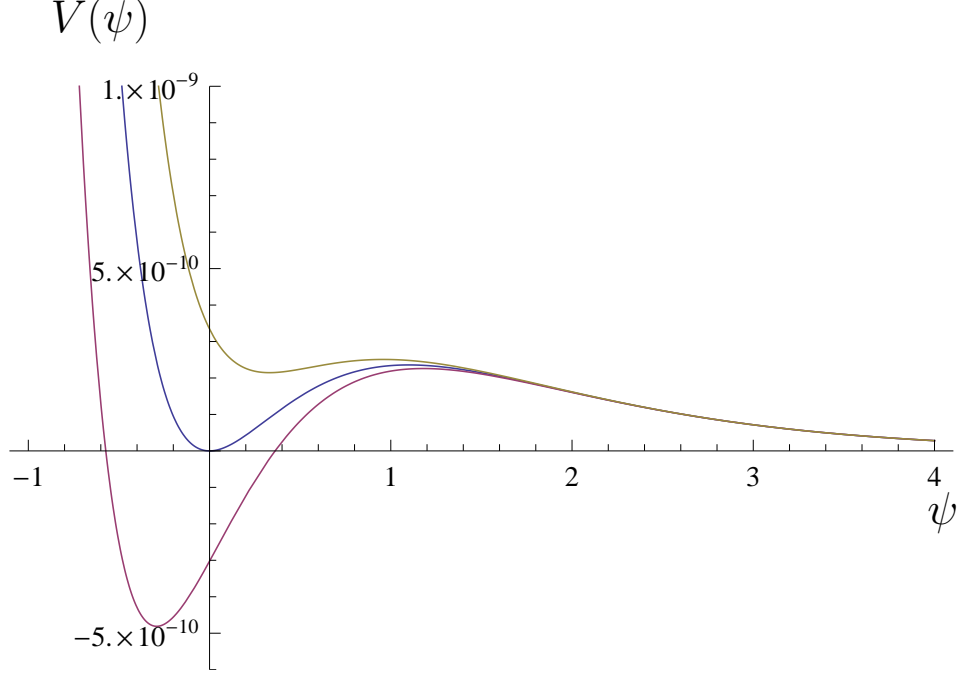


FIG. 1. Plot of the 4d effective potential, in units of M_4^4 , as a function of the field ψ . We show the potential for 3 different values of the flux quantum $n = 180, 200, 220$. The rest of the parameters of the model are fixed to $e^2 = 2$ and $\Lambda_6 = 10^{-4}$, so $n_0 = 200$.

No vacuum solutions exist for $n > n_{max} = 2n_0/\sqrt{3}$. The corresponding value of Q_m is

$$Q_{max}^{(m)} = 4\pi \left(\frac{2}{3\Lambda_6} \right)^{1/2}. \quad (12)$$

A large landscape is possible only if $n_0 \gg 1$, or equivalently $\Lambda_6 \ll e^2$.

Finally, in the $q = 4$ sector the Maxwell field takes the form

$$F_{\mu\nu} = \frac{Q_e}{A_4 R^4} \sqrt{-g_2} \epsilon_{\mu\nu}. \quad (13)$$

where R is the radius of the 4-sphere compactification manifold, $A_4 = 8\pi^2/3$ is the 4-volume of a unit 4-sphere, and $\sqrt{-g_2} = \sqrt{-\tilde{g}_{\mu\nu}}$ is the determinant of the metric in the 2 large dimensions. The charge Q_e is quantized in terms of the elementary charge e by the relation

$$Q_e = ne. \quad (14)$$

One can also represent this sector as a flux compactification model in the dual formulation in terms of a 4-form flux. This is discussed in Appendix A.

We can now look for solutions of our model where the spacetime described by the large 2 dimensions is characterized by a constant scalar curvature, $R^{(2)} = 2H^2$. Einstein's equations

then reduce to the following relations:

$$H^2 = \frac{\Lambda_6}{2} \left(1 - \frac{3Q_e^2}{2A_4^2\Lambda_6 R^8} \right), \quad (15)$$

$$\frac{3}{R^2} = \frac{\Lambda_6}{2} \left(1 + \frac{Q_e^2}{2A_4^2\Lambda_6 R^8} \right). \quad (16)$$

Solutions of these equations are discussed in Appendix B. For $n > n_{max} = (9A_4/e)(3/2\Lambda_6)^{3/2}$, there are no solutions. For $n < n_{max}$, there are two solutions, one with a positive and the other with a negative value of H^2 . (This situation is similar to that in the $q = 2$ sector, where we also have two solutions, one corresponding to a minimum and the other to a maximum of the potential. In both cases, the higher-energy solutions are unstable; see the discussion in Sec.III). As n is increased, the two solutions approach one another, until they both reach $H = 0$ at $n = n_{max}$. The corresponding maximum value of Q_e is given by

$$Q_{max}^{(e)} = 24\pi^2 \left(\frac{3}{2\Lambda_6} \right)^{3/2}. \quad (17)$$

Once again, we can obtain an effective $2d$ theory by integrating out the extra dimensions. The resulting action is that of a $2d$ dilatonic gravity. The action cannot be reduced to the form (6), with Einstein gravity plus a minimally coupled scalar, essentially because the Einstein Lagrangian is a pure divergence in $2d$. Since the ‘‘dilaton’’ field ψ has a non-minimal coupling to gravity, the radius of the compact dimensions cannot be found by simply finding the extrema of the dilaton potential but one can nevertheless identify the solutions presented above as solutions of the scalar tensor theory in $1 + 1$ dimensions.

To summarize, we have found that the landscape of vacua in our theory includes a dS_6 vacuum, a number of dS_4 and AdS_4 vacua with extra dimensions compactified on S_2 , and a number of AdS_2 vacua with extra dimensions compactified on S_4 . We expect that quantum transitions should occur from dS_6 and $dS_4 \times S_2$ vacua to all other vacua, resulting in an eternally inflating multiverse. The AdS vacua are terminal, in the sense that all AdS regions collapse to a big crunch singularity.

Transitions between $dS_4 \times S_2$ vacua with different flux quantum numbers n were discussed in Ref. [7], where it was shown that such transitions proceed through nucleation of magnetically charged branes. The theory does have black brane solutions with the necessary properties [14, 15]. Our focus in the present paper is on the topology-changing transitions. As we shall see, such transitions also involve nucleation of charged black branes or black holes.

III. FROM dS_6 TO $(A)dS_2 \times S_4$

A. The instanton

As discussed in Ref. [8], transitions from dS_6 to $AdS_2 \times S_4$ can be mediated by nucleation of black holes in dS_6 . The corresponding instanton is the Euclideanized 6d Reissner-Nordstrom-de Sitter (RNdS) solution [16],

$$ds^2 = f(r)d\tau^2 + f(r)^{-1}dr^2 + r^2d\Omega_4^2, \quad (18)$$

where

$$f(r) = 1 - \frac{2\tilde{M}}{r^3} + \frac{\tilde{Q}^2}{r^6} - H_6^2 r^2. \quad (19)$$

Here,

$$H_6 = \sqrt{\frac{\Lambda_6}{10}} \quad (20)$$

is the expansion rate of dS_6 , \tilde{M} is the mass parameter, and \tilde{Q} is related to the black hole charge Q_e as

$$Q_e = \sqrt{12}A_4\tilde{Q}. \quad (21)$$

The electric field is given by

$$F_{\tau r} = \frac{iQ_e}{A_4 r^4}, \quad (22)$$

and Q_e is quantized in units of the elementary charge, as in Eq. (14).³

Zeros of the function $f(r)$ correspond to horizons in the Lorentzian solution. There are generally three horizons: the inner (r_-) and outer (r_+) black hole horizons and the cosmological horizon r_c . The range of the variable r in (18) is

$$r_+ \leq r \leq r_c, \quad (24)$$

so that the metric is positive-definite and non-singular, with

$$f(r_+) = f(r_c) = 0. \quad (25)$$

The Euclidean time τ is a cyclic variable with a period chosen to eliminate conical singularities at $r = r_+, r_c$.

³ This is based on the definition of the charge as the integral of the flux through the S_4 sphere around the pointlike charged object

$$Q = \int F_{\tau r} r^4 \sin^3 \theta \sin^2 \phi \sin \psi d\theta d\phi d\psi \quad (23)$$

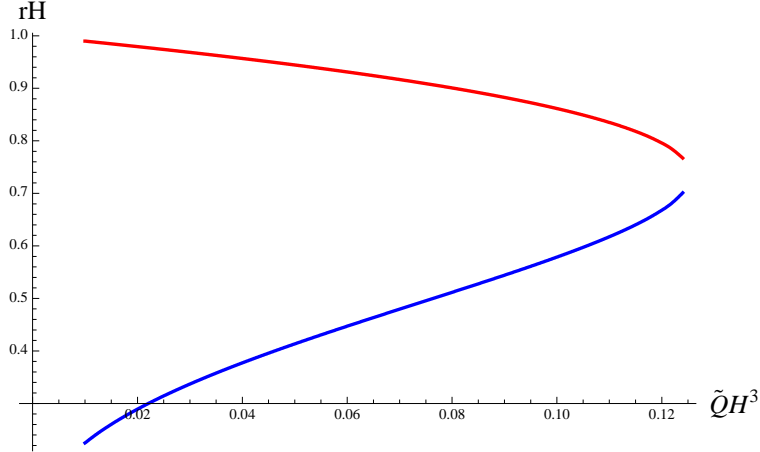


FIG. 2. Plot of r_+H_6 (bottom) and r_cH_6 (top) vs. $\tilde{Q}H_6^3$.

Nucleation of charged black holes in dS space has been extensively studied, both in $4d$ [17–19] and in higher dimensions [20]. For relatively small values of \tilde{Q} , the relevant instantons have the topology of $S_2 \times S_4$, and the avoidance of a conical singularity in the geometry imposes the condition

$$|f'(r_+)| = |f'(r_c)|. \quad (26)$$

The period of τ is then

$$\Delta\tau = \frac{4\pi}{|f'(r_c)|}. \quad (27)$$

These are the so-called “lukewarm instantons”.

The condition (26) implies that the black hole and cosmological horizons have the same temperature and imposes a relation between the parameters \tilde{M} , \tilde{Q} , and H_6 . In our case, H_6 and e should be regarded as fixed by the model, while \tilde{M} is an adjustable parameter. The horizon radii r_+ and r_c are plotted in Fig. 2 as functions of the charge \tilde{Q} . (More precisely, we plot r_+H_6 and r_cH_6 vs. $\tilde{Q}H_6^3$.) As \tilde{Q} is increased at a fixed H_6 , the black hole horizon radius r_+ grows until it coincides, at $\tilde{Q} \approx 0.125H_6^{-3} \equiv \tilde{Q}_c$, with the cosmological horizon r_c .

In the limit when the black hole is much smaller than the cosmological horizon,

$$r_+ \ll r_c, \quad (28)$$

it follows from Eqs. (25), (26) that, up to the leading corrections in $\tilde{q} \equiv \tilde{Q}H_6^3$, we have

$$\tilde{M} \approx \tilde{Q} \left(1 - \frac{1}{2}\tilde{q}^{2/3} \right), \quad (29)$$

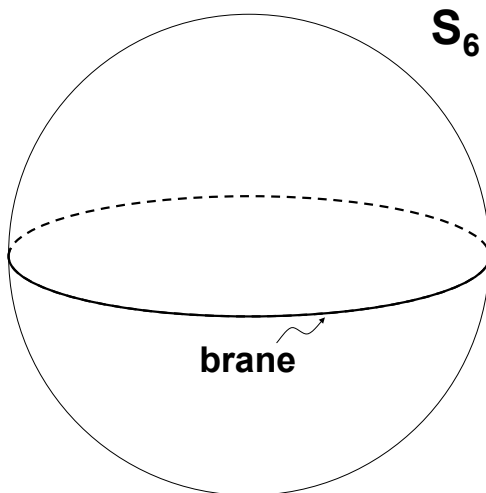


FIG. 3. Topology-change instanton. The charged black hole worldline runs along a big circle on a 6-sphere. The spherical geometry is distorted in the vicinity of the worldline.

$$r_+ \approx \tilde{Q}^{1/3} \left(1 + \frac{1}{3} \tilde{q} \right)^{1/3}, \quad (30)$$

$$r_c \approx H_6^{-1} (1 - \tilde{q}), \quad (31)$$

and

$$\Delta\tau \approx 2\pi H_6^{-1} (1 + 4\tilde{q}). \quad (32)$$

Thus, the instanton in this limit describes the nucleation of nearly extremal black holes in dS_6 . These black holes can be thought of as 0-branes in our theory. The mass M of the black holes can be determined from the behavior of the metric in the range $r_+ \ll r \ll r_c$.

This gives [21]

$$M = \frac{32\pi^2}{3} \tilde{M}. \quad (33)$$

Geometrically, we can picture the RNdS instanton in the following way. Consider the surface $r = r_*$ with $r_+ \ll r_* \ll r_c$. This is a $5d$ surface with topology $S_4 \times S_1$. It encircles the black hole horizon $r = r_+$ with a sphere of radius $r_* \gg r_+$, so that $f(r_*) \approx 1$. Outside of this surface, the metric is that of a 6-sphere, which is the Euclideanized dS_6 . The S_1 comes from the periodic time direction. The length of this circle is given by the period $\Delta\tau$ and is approximately the length of a big circle on S_6 . Thus, the instanton can be pictured as a 0-brane whose worldline runs along a big circle on S_6 , as illustrated in Fig. 3.

Instantons of this form are known to describe the production of particle-antiparticle pairs in de Sitter space [22]. The corresponding instanton action can be estimated as

$$S_{inst} \approx -\frac{16\pi^3}{3H_6^4} + \frac{2\pi M}{H_6}, \quad (34)$$

where the first term is the $6d$ Euclidean de Sitter action, S_{dS_6} , and M is the particle mass. The second term on the right-hand side of (34) is the contribution of the particle worldline action,

$$M \int d\tau. \quad (35)$$

One might also expect to see $O(M)$ corrections to the de Sitter action of a comparable magnitude, caused by distortions of the de Sitter geometry due to the presence of the mass. However, since the action is minimized on the de Sitter solution, the linear in M correction to the action should vanish in the limit of small M .

In our case, the instanton describes nucleation of a pair of oppositely charged black holes with an initial separation of $2H_6^{-1}$. The black holes are then driven apart by the de Sitter expansion. We expect that for $\tilde{q} \ll 1$ the action can be approximated by Eq. (34). Disregarding the pre-exponential factor, the nucleation rate is then given by

$$\Gamma \sim \exp(S_{dS_6} - S_{inst}) \sim \exp(-2\pi M/H_6) \sim \exp\left(\frac{4\pi Q_e}{\sqrt{3} H_6}\right), \quad (36)$$

where in the last step we have used the relations (33), $\tilde{M} \approx \tilde{Q}$, and (21). This agrees with the intuitive expectation that $\Gamma \sim \exp(-M/T_{dS})$, where $T_{dS} = H_6/2\pi$ is the Gibbons-Hawking temperature of dS_6 .⁴

An alternative tunneling channel is given by the so-called charged Nariai instanton, which describes nucleation of maximally large black holes having $r_+ = r_c$ [24, 25]. This instanton has a simple geometry in the form of a product of two round spheres, $S_2 \times S_4$, and is a Euclidean continuation of the $dS_2 \times S_4$ vacuum solution that we discussed in Section II.

The action for lukewarm and charged Nariai instantons in an arbitrary number of dimensions has been calculated in [20]. In the 6-dimensional case we get⁵

$$S_{lukewarm} = 16\pi^2 \Delta\tau \left[-\frac{1}{6} H_6^2 (r_c^5 - r_+^5) + \frac{1}{2} \tilde{Q}^2 (r_+^{-3} - r_c^{-3}) \right] \quad (37)$$

⁴ The nucleation rate can be modified if the action includes a topological term, $S_{top} = -\alpha\chi$, where $\alpha = const$ and χ is the Euler character [23]. In our case, $\chi(S_6) = 2$ and $\chi(S_4 \times S_2) = 4$, so the additional factor in Γ is $e^{2\alpha}$. The same factor would also appear in the nucleation rate of black branes discussed in Section IV.A.

⁵ Note that this expression has been corrected in the latest electronic version of the paper in [20]. We would like to thank Oscar Dias for clarifying this point **10** us.

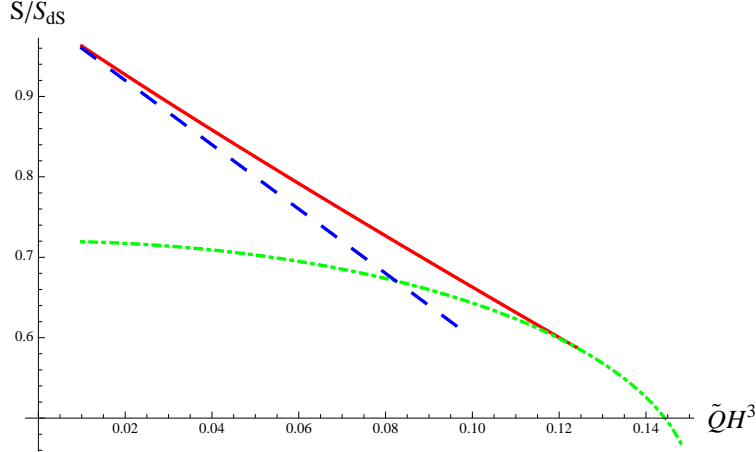


FIG. 4. Plot of S/S_{dS} vs. $\tilde{Q}H_6^3$ for the lukewarm (red/solid line), Nariai (green/dashed-dotted line) and approximate lukewarm (blue/dashed line) actions.

and

$$S_{Nariai} = -\frac{32\pi^3}{3}R^4. \quad (38)$$

where R is the radius of the compact 4-sphere, which can be determined from Eq. (16). The actions (37), (38), in units of the de Sitter action S_{dS_6} , are plotted in Fig. 4 as functions of $\tilde{q} = \tilde{Q}H_6^3$. The lukewarm instanton exists only for $\tilde{Q} < \tilde{Q}_c$, and in all this range its action is smaller⁶ (and thus the nucleation rate is higher) than that for the charged Nariai instanton. As \tilde{Q} approaches \tilde{Q}_c from below, the two instanton actions approach one another and coincide at $\tilde{Q} = \tilde{Q}_c$. The Nariai instanton is the only relevant tunneling channel in the range $\tilde{Q}_c < \tilde{Q} < \tilde{Q}_{max}$,⁷ where $\tilde{Q}_{max} = Q_{max}^{(e)}/\sqrt{12}A_4$ and $Q_{max}^{(e)}$, given by Eq. (17), is the largest value of Q_e above which no instanton solutions exist.

Also shown in Fig. 4 is the approximate action (34). As expected, it is in a good agreement with the exact action at small values of \tilde{Q} . We have also verified this directly, by expanding the lukewarm instanton action (37) at small \tilde{Q} . This gives

$$S_{lukewarm} = -\frac{16\pi^3}{3H_6^4}(1 - 4\tilde{q} + \tilde{q}^{4/3} + \dots), \quad (39)$$

where the neglected terms are $O(\tilde{q}^{5/3})$. The first two terms in this expansion coincide with our approximate formula (34).

⁶ Note that $S_{lukewarm}$ and S_{Nariai} are negative (in addition to $S_{dS_6} < 0$), and that is why in Fig. 4 the graph for the lukewarm action is above that for the Nariai action.

⁷ There is yet another kind of instanton, the so-called “cold” instanton, describing nucleation of extremal Reissner-Nordstrom black holes. Such instantons do not seem to describe compactification transitions, so we do not consider them here.

B. Spacetime structure

To analyze the spacetime structure resulting from the tunneling, we use a Lorentzian continuation of the metric (18), $\tau \rightarrow it$. Introducing a new radial variable ξ as

$$f(r)^{-1/2}dr = d\xi, \quad (40)$$

we have

$$ds^2 = -h(\xi)dt^2 + d\xi^2 + r(\xi)^2 d\Omega_4^2, \quad (41)$$

where $h(\xi) \equiv f(r(\xi))$. We can choose the origin of ξ so that $\xi = 0$ at $r = r_+$. Then, in the vicinity of $r = r_+$ we have

$$h(\xi) \approx \xi^2. \quad (42)$$

We can now continue the metric across the black hole horizon by replacing $\xi \rightarrow it$, $t \rightarrow \xi$,⁸

$$ds^2 = -dt^2 + t^2 d\xi^2 + r_+^2 d\Omega_4^2. \quad (43)$$

This describes an expanding $2d$ FRW universe with 4 extra dimensions compactified on a sphere. The big bang at $t = 0$ is non-singular and corresponds to the horizon at $r = r_+$.

The form (43) applies only in the vicinity of $t = 0$. More generally, the metric behind the horizon can be expressed as

$$ds^2 = -dt^2 + a^2(t)d\xi^2 + r^2(t)d\Omega_4^2, \quad (44)$$

with

$$F_{\mu\nu} = Q_e \frac{a(t)}{A_4 r(t)^4} \epsilon_{\mu\nu} \quad (\mu, \nu = 0, 1). \quad (45)$$

In the limit (28), and at $t \gg r_+$, we expect the metric to approach that of $AdS_2 \times S_4$. The extra dimensions in this metric are stabilized by the electric field; that is why the black holes mediating the topology change need to be charged.

The Penrose diagram for a RNdS black hole is shown in Fig. 5. Region I in the diagram is the region $r_+ < r < r_c$ covered by the static coordinates (41). Region II is the exterior asymptotically de Sitter space, and i_+ is its spacelike future infinity. Region III is the part of the spacetime behind the black hole horizon, which is described by the metric (44). It corresponds approximately to $AdS_2 \times S_4$, with the horizon at r_+ playing the role of the big

⁸ Here we follow the discussion in [8].

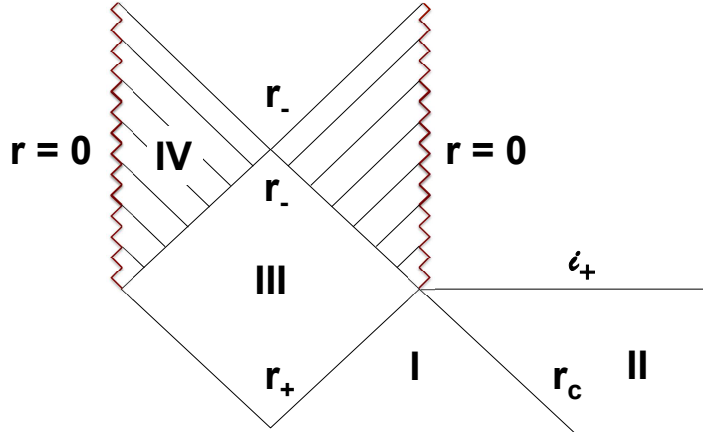


FIG. 5. Penrose diagram for a charged black hole mediating a topology-changing transition $dS_6 \rightarrow AdS_2 \times S_4$. Perturbations result in a singularity at $r = r_-$, so the striped regions are not accessible.

bang and that at r_- the role of the big crunch of the AdS space. In a pure AdS space, both horizons are non-singular, so the black hole is a traversable wormhole, and it is possible for a timelike curve to go from region I across region III into a region similar to I and into another dS_6 space, or to a timelike singularity in region IV. However, if perturbations are included, the horizon at $r = r_-$ develops a true curvature singularity, and the metric cannot be extended beyond region III. A spacelike slice through the topology-changing region is illustrated in a lower-dimensional analogue in Fig. 6.

Thus, we conclude that, from the viewpoint of a $6d$ observer, the topology-changing transitions $dS_6 \rightarrow AdS_2 \times S_4$ look like nucleations of pairs of electrically charged black holes. Each black hole contains an infinite $AdS_2 \times S_4$ universe behind its horizon.

The Lorentzian continuation of the charged Nariai instanton is a $dS_2 \times S_4$ solution, corresponding to one of the positive-energy ($H^2 > 0$) $q = 4$ vacua that we discussed in Section II. These solutions are known to be unstable: small perturbations cause them to disintegrate into $AdS_2 \times S_4$ and dS_6 regions [25].

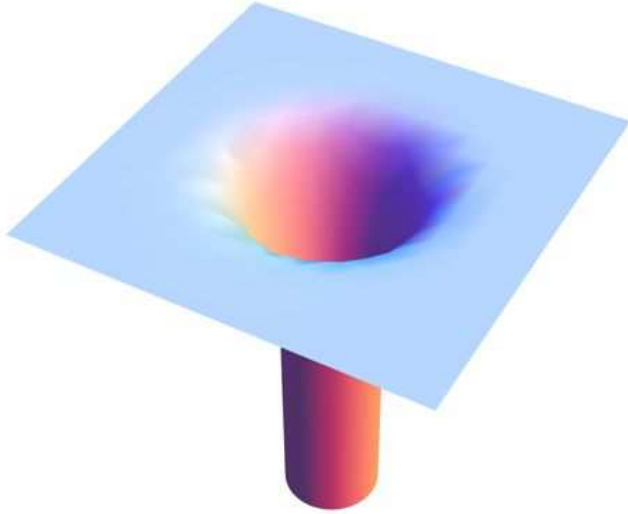


FIG. 6. A spacelike slice through a lower-dimensional analogue of the black hole topology-changing region. In this funnel-like geometry, the flat region at the top has two large dimensions, while the tube of the funnel has one large and one compact dimension.

IV. FROM dS_6 TO $(A)dS_4 \times S_2$

A. The instanton

We shall now argue that topology change from dS_6 to $dS_4 \times S_2$ and to $AdS_4 \times S_2$ can occur through the nucleation of spherical black 2-branes. Since the radius of S_2 is stabilized by magnetic flux, the branes have to be magnetically charged.

It is well known that Einstein-Maxwell theory with $\Lambda_6 = 0$ has magnetically charged, asymptotically flat black brane solutions [14, 15]. In particular, the extreme 2-brane in $6d$ is described by the metric,

$$ds^2 = \left(1 - \frac{r_0}{r}\right)^{2/3} (-dt^2 + dx^2 + dy^2) + \left(1 - \frac{r_0}{r}\right)^{-2} dr^2 + r^2 d\Omega_2^2, \quad (46)$$

with

$$r_0 = \frac{\sqrt{3}Q_m}{8\pi}. \quad (47)$$

The surface $r = r_0$ is a non-singular event horizon. The parameter Q_m in (47) is the quantized magnetic charge (4). The mass per unit area is equal to the brane tension and is

given by [7, 26]

$$T_2 = \frac{2Q_m}{\sqrt{3}}. \quad (48)$$

Note that the metric (46) is invariant with respect to Lorentz boosts in the x and y directions, as expected. Using the results of Refs. [15] and [14], it can be shown that (46) is the only solution which is both non-singular and boost-invariant.

Generalizations of black brane solutions to asymptotically de Sitter background are not known analytically, but can be found numerically, using the ansatz

$$ds^2 = B^2(\xi)[-dt^2 + \exp(2t)(dx^2 + dy^2)] + d\xi^2 + r^2(\xi)d\Omega_2^2, \quad (49)$$

where the coordinates x, y, t can be thought of as brane worldsheet coordinates. Alternatively, one can use the closed de Sitter form of the worldsheet metric,

$$ds^2 = B^2(\xi)[-dt^2 + \cosh^2 t d\Omega_2^2] + d\xi^2 + r^2(\xi)d\Omega_2^2, \quad (50)$$

with the same functions $B(\xi)$ and $r(\xi)$. For a pure dS_6 space, these functions are given by

$$B(\xi) = H_6^{-1} \cos(H_6 \xi), \quad r(\xi) = H_6^{-1} \sin(H_6 \xi), \quad (51)$$

with $\xi = \pi/2H_6$ corresponding to the de Sitter horizon. (This metric covers only part of de Sitter space.)

In the presence of a brane, the Einstein equations for $B(\xi)$ and $r(\xi)$ with the ansatz (3) for the Maxwell field have the form

$$\begin{aligned} \frac{1}{B(\xi)^2} + \frac{1}{r(\xi)^2} - \frac{B'(\xi)^2}{B(\xi)^2} - \frac{4B'(\xi)r'(\xi)}{B(\xi)r(\xi)} - \frac{r'(\xi)^2}{r(\xi)^2} - \frac{2B''(\xi)^2}{B(\xi)} - \frac{2r''(\xi)}{r(\xi)} &= \Lambda + \frac{Q_m^2}{32\pi^2 r(\xi)^4}, \\ \frac{3}{B(\xi)^2} + \frac{1}{r(\xi)^2} - \frac{3B'(\xi)^2}{B(\xi)^2} - \frac{6B'(\xi)r'(\xi)}{B(\xi)r(\xi)} - \frac{r'(\xi)^2}{r(\xi)^2} &= \Lambda + \frac{Q_m^2}{32\pi^2 r(\xi)^4}, \\ \frac{3}{B(\xi)^2} - \frac{3B'(\xi)^2}{B(\xi)^2} - \frac{3B'(\xi)r'(\xi)}{B(\xi)r(\xi)} - \frac{3B''(\xi)}{B(\xi)} - \frac{r''(\xi)}{r(\xi)} &= \Lambda - \frac{Q_m^2}{32\pi^2 r(\xi)^4}. \end{aligned} \quad (52)$$

The first of these equations follows from the other two, so there are two independent equations for the two functions, $B(\xi)$ and $r(\xi)$.

Before discussing the solutions of these equations, let us consider a Euclidean continuation of the metric (50). This can be found by setting $t = i\theta - i\pi/2$,

$$ds^2 = B^2(\xi)d\Omega_3^2 + d\xi^2 + r^2(\xi)d\Omega_2^2. \quad (53)$$

We are interested in compact, non-singular instanton solutions, so the range of ξ has to be finite, $0 < \xi < \xi_m$, with the endpoints corresponding to zeros of $B(\xi)$,

$$B(0) = B(\xi_m) = 0. \quad (54)$$

These endpoints are non-singular, provided that

$$B'(0) = B'(\xi_m) = 1 \quad (55)$$

and

$$r'(0) = r'(\xi_m) = 0. \quad (56)$$

The boundary conditions (54)-(56) select a unique solution of Eqs. (52). For specified values of H_6 and Q_m , the solution can be found numerically. For small values of Q_m ,

$$Q_m \ll H_6^{-1}, \quad (57)$$

the brane horizon radius is much smaller than that of the cosmological horizon at $\xi_m \approx \pi/2H_6$, and we expect the solution to be well approximated by the spherical metric (51), except in the vicinity of $\xi = 0$. We also expect that in this limit the brane horizon radius is $r(0) \approx r_0$ with r_0 from (47) and the brane tension is approximately given by (48).

In Figs. 7 and 8 we find the numerical solution for the case $e^2 = 2$, $\Lambda_6 = 10^{-4}$ and $n = 10$. This value of n corresponds to a small magnetic charge so one can see from the figures that the functions only deviate slightly from their pure de Sitter counterparts. In Fig. 9 we show a close up of the region near the black brane horizon and compare the asymptotic value of r with the analytic estimate in the small charge regime, namely, r_0 from Eq. (47).

Analysis similar to that in Sec. III.A indicates that the black brane instanton can be pictured as a 2-brane, whose worldsheet has the form of a 3-sphere and is wrapped around a ‘‘big circle’’ of S_6 , as illustrated in Fig. 3. As discussed in [22], such instantons describe spontaneous nucleation of horizon-radius spherical branes in de Sitter space. The instanton action in the limit (57) can be estimated as

$$S_{inst} \approx S_{dS_6} + A_3 H_6^{-3} T_2, \quad (58)$$

where $A_3 = 2\pi^2$ is the volume of a unit 3-sphere and T_2 is the tension of the brane given by (48). As for the black hole instanton, the presence of the brane does not induce any linear

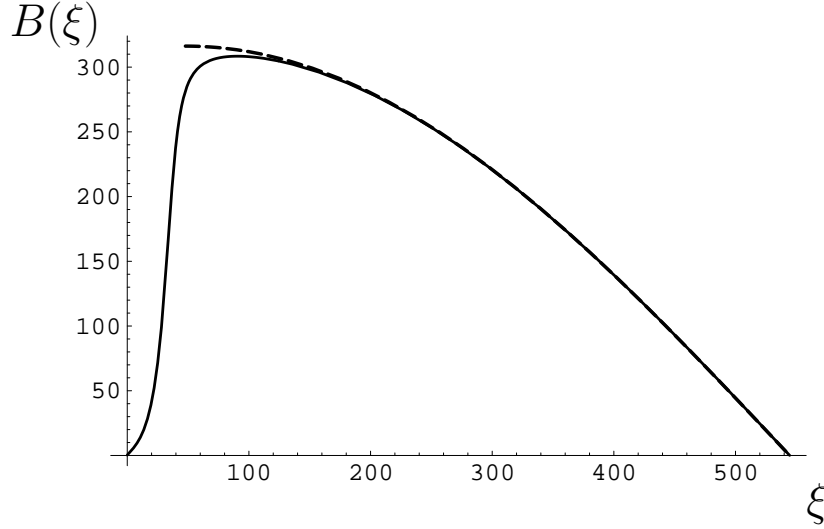


FIG. 7. Numerical solution for the function $B(\xi)$ for the magnetically charged inflating brane (solid line). We show for comparison the pure de Sitter solution Eq. (51) shifted to match the numerical solution at the cosmological horizon endpoint, namely ξ_m (dashed line). We use here the parameters specified in Fig. 1 and the brane solution corresponds to the case $n = 10$.

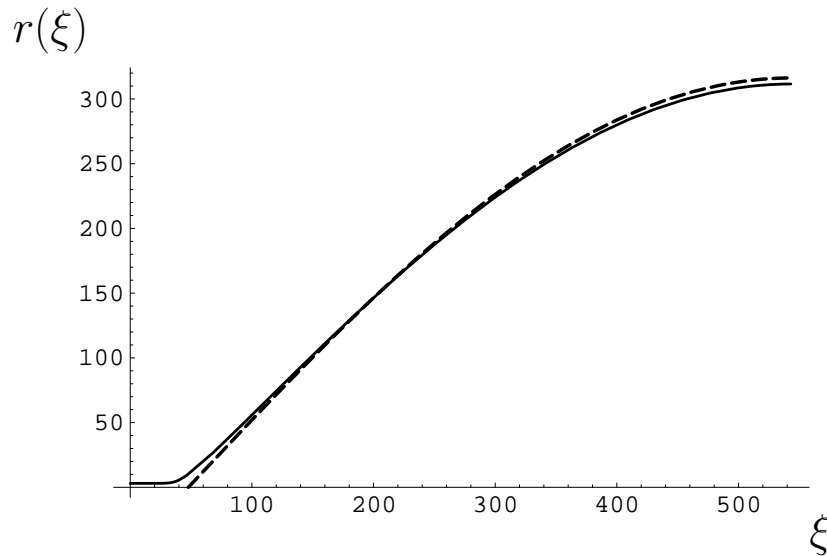


FIG. 8. Numerical solution for the function $r(\xi)$ (solid line) for the same parameters as in Figure 7. The dashed line is the solution for $r(\xi)$ for the pure dS_6 case, Eq. (51). Note that we have shifted the pure de Sitter solution to make the cosmological horizon coincide with ξ_m .

in T_2 corrections to S_{dS_6} , because dS_6 is a minimum of the action. The brane nucleation rate is given by

$$\Gamma \sim \exp(-2\pi^2 H_6^{-3} T_2). \quad (59)$$

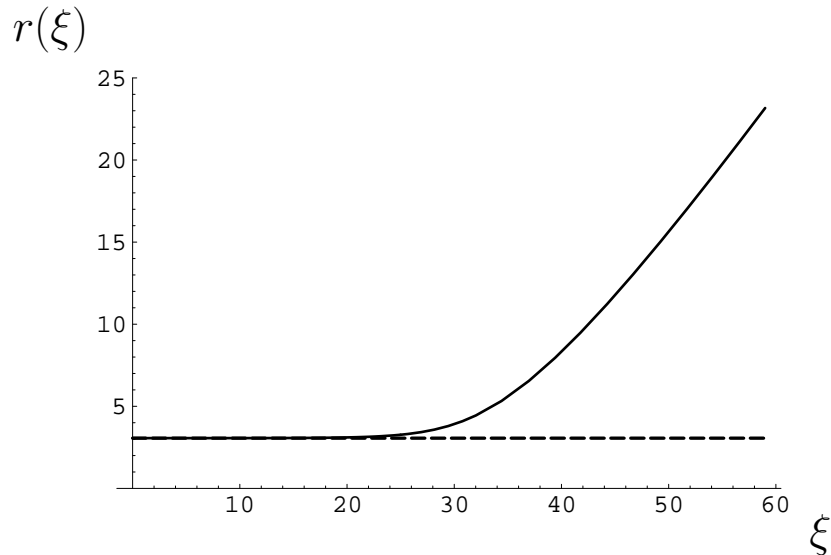


FIG. 9. Magnified plot of the numerical solution in Fig. 8 for $r(\xi)$ near the brane horizon (solid line). We also show for comparison the analytic estimate of the brane horizon for this particular brane solution (dashed line) given by Eq. (47).

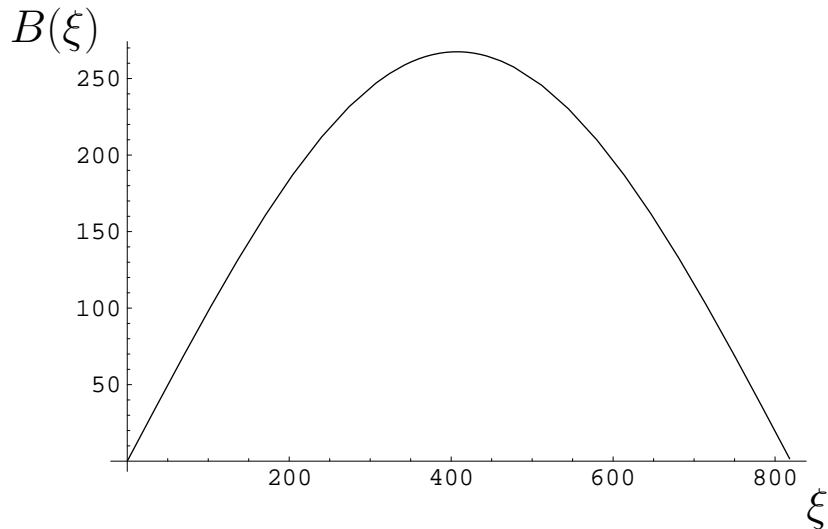


FIG. 10. Numerical solution for the function $B(\xi)$ for the magnetically charged inflating brane solution with $n = 200$.

We note that it follows from Eq. (10) that for small values of Q_m satisfying (57) the $4d$ cosmological constant is necessarily negative. For $Q_m \sim H_6^{-1}$, the brane and cosmological horizons are comparable to one another, and the metric significantly differs from (51) all the way to $r = r_c$. In this regime, the instanton action needs to be calculated numerically. An example in this regime is shown in Figs. 10 and 11.

The tunneling process can also be described using the $4d$ effective theory. The instanton

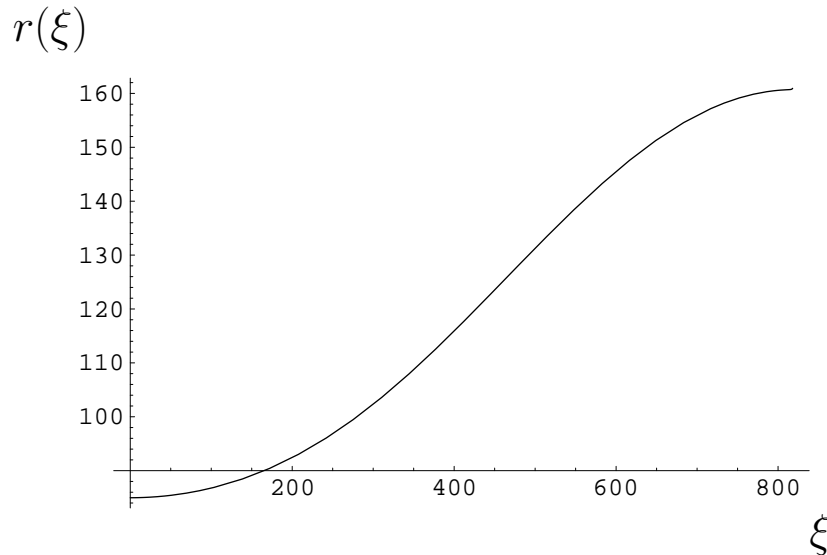


FIG. 11. Numerical solution for the function $r(\xi)$ for the case $n = 200$.

is then the usual Coleman-De Luccia (CdL) instanton. This description was used by Carroll, Johnson and Randall (CJR) [8] and is equivalent to ours, but the geometry of the instanton and the resulting spacetime structure are not evident in this approach. CJR performed a numerical calculation of the instanton action as a function of the magnetic charge Q_m ; the result is shown in their Fig. 17. We have verified that their calculation agrees with our approximate formula (58). Since the graph obtained by CJR is nearly a straight line, our formula gives a good approximation in the entire range of Q_m .

CJR have also considered a Nariai-type instanton and compared its action to that of the CdL-type instanton. In the present case, the Nariai-type instanton is the Euclideanized unstable $dS_4 \times S_2$ vacuum solution, corresponding to the maximum of $V(\psi)$. Its action is greater than that for the black brane instanton discussed above for all values of Q_m , up to some critical value $Q_c^{(m)}$ at which the two actions coincide⁹. The black brane instanton does not exist for $Q_m > Q_c^{(m)}$, and no instanton solutions exist for $Q_m > Q_{max}^{(m)}$ with $Q_{max}^{(m)}$ given by Eq. (12). The value of $Q_c^{(m)}$ depends non-trivially on Λ_6 .

⁹ One can see how the inflating black brane solutions approach the Nariai limiting case by looking at the numerical solutions presented in Figs. 10 and 11. This is an intermediate solution where the function $B(\xi)$ approaches a pure sine function and $r(\xi)$ has a small variation from r_+ to r_c as one would expect for a near Nariai solution.

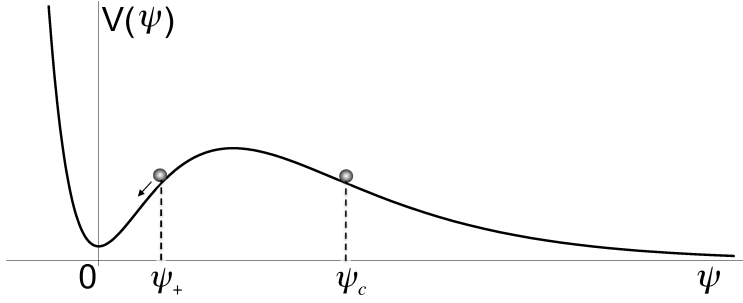


FIG. 12. Scalar field potential of the effective 4d theory. In the newly formed compactified region, ψ starts at ψ_+ and rolls to $\psi = 0$.

B. Spacetime structure

Let us now analyze the spacetime structure resulting from brane nucleation. The region between the brane horizon, $\xi = 0$, and the cosmological horizon, $\xi = \xi_m$, is described by the metric (50). Surfaces of constant ξ in this metric have the geometry of $dS_3 \times S_2$, indicating that the brane worldsheet is effectively an expanding 3d de Sitter space. In the vicinity of the brane horizon at $\xi = 0$, we have $B(\xi) \approx \xi$ and $r(\xi) \approx r_+$, where $r_+ = r(0)$ is the brane horizon radius,

$$ds^2 = \xi^2(-dt^2 + \cosh^2 t d\Omega_2'^2) + d\xi^2 + r_+^2 d\Omega_2^2. \quad (60)$$

Analytic continuation across the horizon is obtained by replacing $\xi \rightarrow it$, $t \rightarrow \chi + i\pi/2$.

This gives

$$ds^2 = -dt^2 + t^2 d\mathcal{H}_3^2 + r_+^2 d\Omega_2^2, \quad (61)$$

where

$$d\mathcal{H}_3^2 = d\chi^2 + \sinh^2 \chi d\Omega^2 \quad (62)$$

is a 3d hyperbolic metric of unit curvature radius. The metric (61) describes an expanding, open 4d FRW universe with 2 extra dimensions compactified on a sphere.

The metric (61) applies only in the vicinity of $t = 0$, where the 4d universe is curvature-dominated. More generally, the metric behind the black brane horizon has the form

$$ds^2 = -dt^2 + a^2(t) d\mathcal{H}_3^2 + r^2(t) d\Omega_2^2. \quad (63)$$

The evolution of $a(t)$ and $r(t)$ can be found by numerically solving the Lorentzian version of the 6d Einstein equations. Alternatively, we can use the effective 4d theory (6). The 4d

metric is given by

$$ds_4^2 = -d\tilde{t}^2 + \tilde{a}^2(\tilde{t})d\mathcal{H}_3^2 \quad (64)$$

and the scalar field ψ is a function of \tilde{t} only. The $4d$ and $6d$ descriptions are connected by the relations

$$dt = e^{-\psi(\tilde{t})/2M_4} d\tilde{t}, \quad (65)$$

$$a(t) = e^{-\psi(\tilde{t})/2M_4} \tilde{a}(\tilde{t}), \quad (66)$$

$$r(t) = R e^{\psi(\tilde{t})/2M_4}. \quad (67)$$

The $4d$ evolution equations have the form

$$\ddot{\psi} + 3\frac{\dot{\tilde{a}}}{\tilde{a}}\dot{\psi} + V'(\psi) = 0, \quad (68)$$

$$\left(\frac{\dot{\tilde{a}}}{\tilde{a}}\right)^2 - \frac{1}{\tilde{a}^2} = \frac{1}{3M_4^2} \left(\frac{\dot{\psi}^2}{2} + V(\psi)\right), \quad (69)$$

where dots stand for derivatives with respect to \tilde{t} and $V(\psi)$ given by (7).

From a $4d$ point of view, our tunneling process is the usual Coleman-De Luccia (CdL) tunneling through the barrier in the potential $V(\psi)$. The field values ψ_c and ψ_+ , corresponding respectively to r_c and r_+ are located on the opposite sides of the barrier (see Fig. 12). The evolution starts at $\tilde{t} = 0$ with $\psi = \psi_+$ and $\tilde{a} = 0$, and the field ψ starts rolling towards the potential minimum at $\psi = 0$. The long-term evolution depends on whether this minimum has positive or negative energy density. For $\Lambda_4 < 0$, we have an $AdS_4 \times S_2$ vacuum, and the evolution ends in a singular big crunch, while for $\Lambda_4 > 0$, the evolution is non-singular and the metric asymptotically approaches a $4d$ de Sitter space with $\psi \rightarrow 0$. The corresponding spacetime diagrams are shown in Fig. 13.

Nariai-type instantons are similar to Hawking-Moss instantons [27]. As discussed in [8], they describe nucleation of regions of size comparable to the horizon, filled with the unstable vacuum at the maximum of $V(\psi)$. Small perturbations will cause ψ to roll away from the maximum. As a result, the newly formed region will either disintegrate into dS_6 and $(A)dS_4 \times S_2$ domains, or, if the potential $V(\psi)$ is sufficiently flat near the maximum, it will become a site of eternal inflation, with dS_6 and $(A)dS_4 \times S_2$ sub-regions constantly being formed.

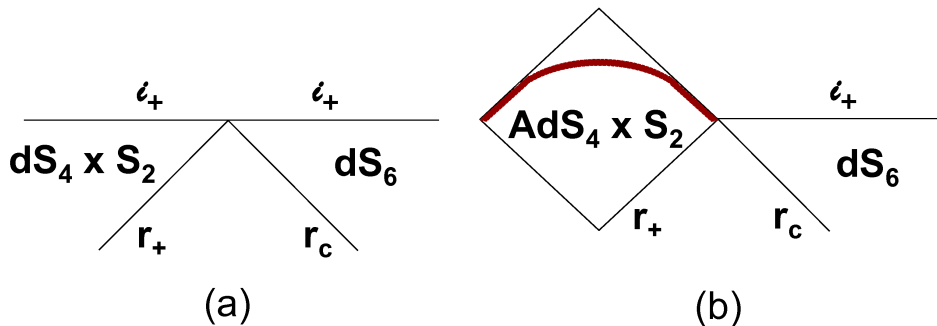


FIG. 13. Spacetime diagrams for transitions from dS_6 to $dS_4 \times S_2$ (a) and $AdS_4 \times S_2$ (b).

V. FROM $dS_4 \times S_2$ TO dS_6

The decompactification transition from $dS_4 \times S_2$ to dS_6 has been discussed in Refs. [7, 8]. In terms of the effective 4D theory, this is the usual false vacuum decay. A bubble with $\psi \sim \psi_c$ nucleates in the inflating background of $\psi = 0$ vacuum. As the bubble expands, the field rolls off to infinity in the bubble interior. The tunneling is described by the same CdL instanton as for the inverse transition, $dS_6 \rightarrow dS_4 \times S_2$, and the tunneling rate is

$$\Gamma \sim \exp(S_0 - S_{inst}), \quad (70)$$

where

$$S_0 = -24\pi^2 M_4^4 / \Lambda_4, \quad (71)$$

with M_4 and Λ_4 from Eqs. (8) and (10), respectively. The rate (70) has been estimated in [7] and has been calculated numerically for different values of parameters in Ref. [8].

The 4d evolution after tunneling is described by the same equations (68), (69) as for the inverse transition, except now the evolution starts with $\psi(\tilde{t} = 0) = \psi_c$ and the field ψ rolls towards $\psi = \infty$, so the extra dimensions become large. The role of the bubble wall is played by the expanding black 2-brane. A spacelike slice through the decompactification bubble spacetime is illustrated in Fig. 14.

The 6-dimensional metric in the bubble interior has the form (63). At late times, $t \rightarrow \infty$, the metric approaches that of dS_6 [6], with $a(t) \approx H_6^{-1} \sinh(H_6 t)$ and $r(t) \approx H_6^{-1} \cosh(H_6 t)$. This is a somewhat unfamiliar, “mixed” slicing of de Sitter space, with open slices in 3 out of 5 spatial dimensions and closed spherical slices in the remaining two directions. The compact dimensions always remain compact, but asymptotically become very large, and the

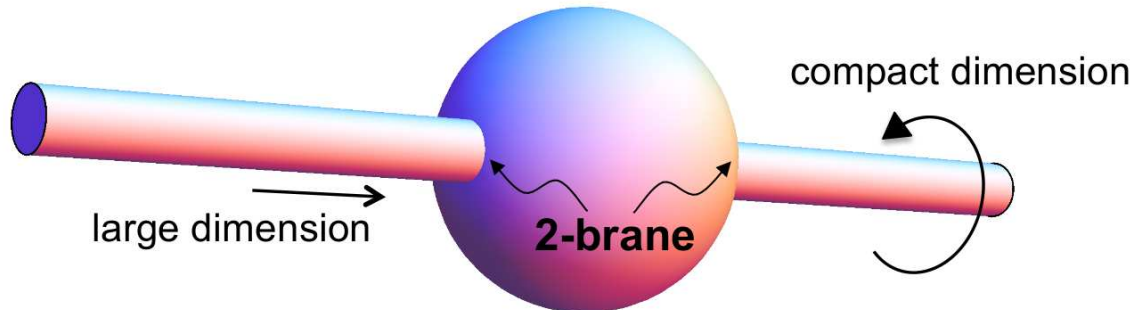


FIG. 14. A spatial slice through the decompactification bubble spacetime. The junctions marked as “2-branes” in this lower-dimensional analogue become a 2-sphere in $5d$.

metric becomes locally isotropic in the limit.

VI. CONCLUSIONS

The Einstein-Maxwell theory in 6 dimensions admits a rich landscape of vacua and provides a useful toy model for investigating the dynamics of the multiverse. The landscape of this theory includes a dS_6 vacuum, a number of dS_4 and AdS_4 vacua with extra dimensions compactified on S_2 , and a number of AdS_2 vacua with extra dimensions compactified on S_4 . There are also some perturbatively unstable $dS_4 \times S_2$ and $dS_2 \times S_4$ vacua. In this paper we studied quantum tunneling transitions between vacua of different effective dimensionality. We identified the appropriate instantons and described the spacetime structure resulting from the tunneling. Our results reinforce and extend the earlier analyses in Refs. [8] and [7].

We found that compactification transitions from dS_6 to $AdS_2 \times S_4$ occur through nucleation of pairs of electrically charged black holes. The charge of these black holes is quantized in units of the elementary charge of the theory, and their mass is determined by the condition that the temperature at the black hole horizon ($r = r_+$) is the same as that at the cosmological horizon ($r = r_c$) in the corresponding Reissner-Nordstrom-de Sitter solution. These black holes can be thought of as 0-branes of the theory. In the limit when $r_+ \ll r_c$ the black holes become nearly extremal. The instanton in this limit can be pictured as S_6 (Euclideanized de Sitter) with a 0-brane worldline running along a big circle.

Transitions from dS_6 to $dS_4 \times S_2$ and $AdS_4 \times S_2$ proceed through nucleation of spherical, magnetically charged black 2-branes. Once again, in the limit when the black brane horizon radius r_+ is small compared to r_c , the corresponding instanton can be pictured as a brane whose Euclidean worldsheet (which has the form of a 3-sphere) is wrapped around a “big circle” of S_6 . The process of black brane formation through quantum tunneling is very similar to nucleation of spherical domain walls during inflation, which was analyzed in Ref. [22].

The initial radius of a nucleating brane is set by the de Sitter horizon, H_6^{-1} . Once the brane is formed, this radius is stretched by the exponential expansion of the universe, while the transverse dimension of the brane (which can be identified with its horizon radius r_+) remains fixed. Behind the horizon, in the black brane interior, the spacetime is effectively 4-dimensional, with the extra two dimensions compactified on S_2 . Observers in this newly formed compactified region see only a homogeneous FRW universe, approaching either dS or AdS space.

Transitions from dS_6 to unstable $dS_2 \times S_4$ (or $dS_4 \times S_2$) vacua are mediated by Nariai-type instantons, which are similar to Hawking-Moss instantons. Small perturbations cause fragmentation of these vacua into regions of $AdS_2 \times S_4$ (or $AdS_4 \times S_2$) and dS_6 .

We also discussed decompactification transitions $dS_4 \times S_2 \rightarrow dS_6$, in which the effective dimension of the daughter vacuum is higher than that of the parent vacuum. These transitions are described by the same instanton as the inverse process, $dS_6 \rightarrow dS_4 \times S_2$, but the resulting spacetime structure is rather different. Observers in the parent vacuum see nucleation and subsequent expansion of spherical bubbles, as in ordinary CdL vacuum decay. The role of the bubble wall is played by a spherical magnetically charged black brane (the same kind of brane as in the inverse transition). The bubble interior is initially anisotropic, but as the compact dimensions expand, it approaches local isotropy, with the metric approaching the $6d$ de Sitter space. However, the anisotropy may still be observable in the CMB if inflation inside the bubble terminates after a relatively small number of e -foldings. These issues will be discussed separately in [28].

Apart from the topology-changing transitions that we discussed here, our model admits tunneling transitions between $(A)dS_4 \times S_2$ vacua having the same topology, but characterized by different values of the magnetic flux. Such tunnelings, which are analogous to the Schwinger process, and the corresponding instantons, have been discussed in [7]. The role of the bubble walls in the resulting bubbles is played by magnetically charged branes,

which can be either solitonic branes (if the model is augmented by adding the appropriate Higgs fields) or black branes of the type described here. In the latter case, the region inside the black brane horizon is a new $(A)dS_4 \times S_2$ universe. Thus, the tunneling results in the formation of two compactified regions: one in the interior of the expanding bubble, where the flux has been changed with respect to the parent vacuum, and the other in the interior of the black brane itself.

Topology-changing transitions of the kind we discussed in this paper will inevitably occur in the course of eternal inflation. As a result, the multiverse will be populated by vacua of all possible dimensionalities. A spacelike slice through such a multiverse might look like Linde’s famous “cactus” picture [29]; its version adapted for our present model is shown in Fig. 15. We shall discuss the structure of this multi-dimensional multiverse and its implications for the measure problem in a separate paper.

Finally, as Fig. 15 suggests, we expect that there should be other kinds of instantons that interpolate directly between the $dS_4 \times S_2$ and $AdS_2 \times S_4$ sectors in our model. These would be somewhat more complicated solutions that will not only change the topology of spacetime, but would also act as sources and sinks for the different fluxes involved.

VII. ACKNOWLEDGMENTS

We are grateful to Raphael Bousso, Oscar Dias, Jaume Garriga, Andrei Linde, Maulik Parikh, Oriol Pujolas, Mike Salem and Ben Shlaer for very helpful discussions. J.J. B.- P. would like to thank the Theory division at CERN for their support and hospitality while part of this work was being completed. This work was supported in part by the National Science Foundation Grants 06533561 (J.J.B-P.) and 0353314 (A.V.).

Appendix A: The Electric Sector in the four form language

In this appendix we will discuss 6 dimensional Einstein gravity coupled to a 4-form field. We will call this the electric sector of the $6d$ model. In this case we have 2 large dimensions and 4 compact ones. The Lagrangian is given by

$$S = \int d^6x \sqrt{-\tilde{g}} \left(\frac{1}{2} \tilde{R}^{(6)} - \frac{1}{48} F_{MNPQ} F^{MNPQ} - \Lambda_6 \right), \quad (\text{A1})$$

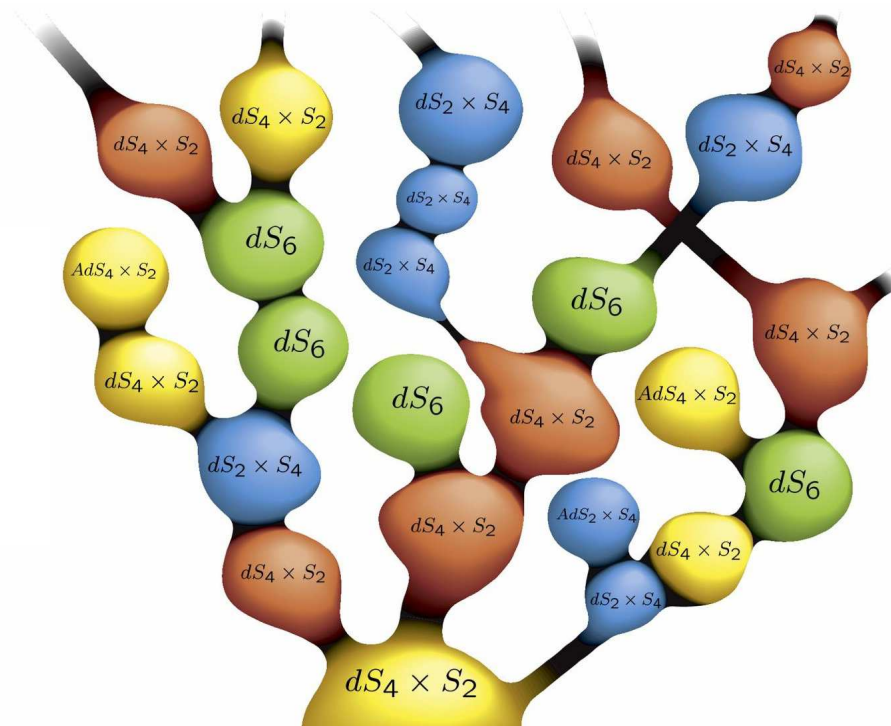


FIG. 15. A spacelike slice through a multi-dimensional multiverse. The dark regions represent black holes and black branes. This is an adaptation of Andrei Linde's picture in [29].

which is the dual theory of the electromagnetic formulation given in the main part of the text. The corresponding field equations are

$$\tilde{R}_{MN}^{(6)} - \frac{1}{2}\tilde{g}_{MN}\tilde{R}^{(6)} = T_{MN} \quad (\text{A2})$$

and

$$\frac{1}{\sqrt{-\tilde{g}}}\partial_M \left(\sqrt{-\tilde{g}}F^{MNPQ} \right) = 0, \quad (\text{A3})$$

with the energy-momentum tensor given by

$$T_{MN} = \frac{1}{4!} \left(4F_{MPQR}F_N^{PQR} - \frac{1}{2}\tilde{g}_{MN}F^2 \right) - \tilde{g}_{MN}\Lambda_6. \quad (\text{A4})$$

We will look for solutions of this model with the spacetime metric given by a two-dimensional maximally symmetric space of constant curvature,¹⁰ $R^{(2)} = 2H^2$, and a static extra-dimensional 4-sphere of fixed radius, namely a metric of the form

$$ds^2 = \tilde{g}_{MN}dx^M dx^N = \tilde{g}_{\mu\nu}dx^\mu dx^\nu + R^2 d\Omega_4^2. \quad (\text{A5})$$

¹⁰ As before, H^2 can be positive or negative, depending on whether we are talking about de Sitter or anti-de Sitter spaces.

With this ansatz, we obtain the following components of the $6d$ Einstein tensor:

$$\tilde{G}_{\mu\nu}^{(6)} = -\frac{6}{R^2} \tilde{g}_{\mu\nu}, \quad (\text{A6})$$

$$\tilde{G}_{ab}^{(6)} = -\left(H^2 + \frac{3}{R^2}\right) \tilde{g}_{ab}, \quad (\text{A7})$$

where we have used μ and ν to denote the two dimensional coordinates and a and b run over the four extra dimensions on the sphere.

The field strength is taken to be proportional to the volume form on S_q , namely,

$$F_{\theta\phi\psi\chi} = \frac{Q_e}{A_4} (\det g_{ab})^{1/2} = \frac{Q_e}{A_4} \sin^3 \theta \sin^2 \phi \sin \psi, \quad (\text{A8})$$

which gives rise to the following energy-momentum tensor

$$T_{\mu\nu} = -\tilde{g}_{\mu\nu} \left(\frac{Q_e^2}{2A_4^2 R^8} + \Lambda_6 \right) \quad (\text{A9})$$

and

$$T_{ab} = \tilde{g}_{ab} \left(\frac{Q_e^2}{2A_4^2 R^8} - \Lambda_6 \right), \quad (\text{A10})$$

where, as before,

$$Q_e = ne. \quad (\text{A11})$$

Equating the Einstein tensor and the stress-energy tensor we find

$$H^2 = \frac{\Lambda_6}{2} \left(1 - \frac{3Q_e^2}{2A_4^2 \Lambda_6 R^8} \right) \quad (\text{A12})$$

and

$$\frac{3}{R^2} = \frac{\Lambda_6}{2} \left(1 + \frac{Q_e^2}{2A_4^2 \Lambda_6 R^8} \right). \quad (\text{A13})$$

These equations are quartic in R^2 . Upon solving Eq. (A13) for R^2 we find that two of the four solutions yield negative R^2 , and are thus discarded. The solutions are algebraically complicated, and are analyzed in Appendix B. The key point for this study is that for the two viable solutions it can be shown that upon substituting into Eq. (A12) one solution always yields a positive H^2 while the other solution always yields a negative H^2 .

Appendix B: Solving for R^2

We need to solve Eq. (16),

$$\frac{3}{R^2} = \frac{\Lambda_6}{2} \left(1 + \frac{Q_e^2}{2A_4^2 \Lambda_6 R^8} \right). \quad (\text{B1})$$

Multiplying this equation by $(Q_e/A_4)^{2/3}$ and introducing a new variable $x = R/(Q_e/A_4)^{1/3}$, we have

$$\frac{3}{x^2} = \frac{\Lambda_6(Q_e/A_4)^{2/3}}{2} + \frac{1}{4x^8}, \quad (\text{B2})$$

or

$$1 - Kx^2 = \frac{1}{12x^6}, \quad (\text{B3})$$

where

$$K = \frac{(Q_e/A_4)^{2/3}\Lambda_6}{6}. \quad (\text{B4})$$

The function on the l.h.s. of eq. (B3) is convex and the function on r.h.s. is concave. For sufficiently small values of K , there are two roots. As K is increased, the roots approach one another until they coincide at some critical value K_{max} (corresponding to some flux quantum number n_{max}). For $K > K_{max}$, there are no solutions.

The critical value K_{max} can be found by noticing that at this value of K the graphs of the functions on the two sides of eq.(B3) are tangent to one another at the point where they meet. This yields the condition

$$x^8 = \frac{1}{4K}. \quad (\text{B5})$$

Combining this with Eq. (B3), we find

$$K_{max} = \frac{3^{4/3}}{4}. \quad (\text{B6})$$

Using Eqs. (B4), (14) and (15), it can be verified that the corresponding values of Q_e , n and H are

$$Q_{max}^{(e)} = 9A_4 \left(\frac{3}{2\Lambda_6} \right)^{3/2}, \quad (\text{B7})$$

$$n_{max} = \frac{9A_4}{e} \left(\frac{3}{2\Lambda_6} \right)^{3/2}, \quad (\text{B8})$$

and $H = 0$. Since the two solutions of (B1) merge at $H = 0$, it is clear that for $K < K_{max}$ one of these solutions has $H > 0$ and the other $H < 0$.

For $K \ll K_{max}$, the solutions of (B3) can be approximated as

$$x_1 \approx 12^{-1/6}, \quad x_2 \approx K^{-1/2}. \quad (\text{B9})$$

(Note that in this case $K \ll 1$.)

Appendix C: Inflating brane equations of motion

Taking into account the following ansatz for the metric,

$$ds^2 = B^2(\xi)[-dt^2 + \cosh^2 t d\Omega_2^2] + d\xi^2 + r^2(\xi)d\Omega_2^2, \quad (C1)$$

we obtain an Einstein tensor of the form,

$$G_t^t = G_{\theta'}^{\theta'} = G_{\phi'}^{\phi'} = -\frac{1}{B(\xi)^2} - \frac{1}{r(\xi)^2} + \frac{B'(\xi)^2}{B(\xi)^2} + \frac{4B'(\xi)r'(\xi)}{B(\xi)r(\xi)} + \frac{r'(\xi)^2}{r(\xi)^2} + \frac{2B''(\xi)^2}{B(\xi)} + \frac{2r''(\xi)}{r(\xi)},$$

$$G_\xi^\xi = -\frac{3}{B(\xi)^2} - \frac{1}{r(\xi)^2} + \frac{3B'(\xi)^2}{B(\xi)^2} + \frac{6B'(\xi)r'(\xi)}{B(\xi)r(\xi)} + \frac{r'(\xi)^2}{r(\xi)^2},$$

$$G_\theta^\theta = G_\phi^\phi = -\frac{3}{B(\xi)^2} + \frac{3B'(\xi)^2}{B(\xi)^2} + \frac{3B'(\xi)r'(\xi)}{B(\xi)r(\xi)} + \frac{3B''(\xi)}{B(\xi)} + \frac{r''(\xi)}{r(\xi)}.$$

On the other hand, the energy-momentum tensor of the brane in this metric can be computed to be,

$$T_t^t = T_{\theta'}^{\theta'} = T_{\phi'}^{\phi'} = -\Lambda_6 - \frac{Q_m^2}{32\pi^2 r(\xi)^4}$$

$$T_\xi^\xi = -\Lambda_6 - \frac{Q_m^2}{32\pi^2 r(\xi)^4}$$

$$T_\theta^\theta = T_\phi^\phi = -\Lambda_6 + \frac{Q_m^2}{32\pi^2 r(\xi)^4}$$

We require that our solution must be free of singularities at the brane horizon as well as the cosmological horizon, which in turn means that the most general expansion around those points should be of the form

$$\begin{aligned} B(\xi) &= \xi + B_3 \xi^3 + \dots \\ r(\xi) &= r_H + r_2 \xi^2 + \dots \end{aligned} \quad (C2)$$

where we have assumed that the position of the horizon in question is at $\xi = 0$ and its radius is r_H . Plugging this expansion back into the equations of motion we arrive at the following expression for the coefficients B_3 and r_2 in terms of Λ_6 , Q_m and r_H , namely,

$$\begin{aligned} B_3 &= -\frac{4r_H^2 - 5(Q_m/4\pi)^2 + 2r_H^4\Lambda_6}{144r_H^4} \\ r_2 &= \frac{4r_H^2 - 3(Q_m/4\pi)^2 - 2r_H^4\Lambda_6}{32r_H^3}. \end{aligned} \quad (C3)$$

Using this expansion we can now integrate the equations of motion forward in ξ up to the other horizon. The value of r_H is then fixed by imposing the regularity condition on the other horizon.

-
- [1] L. Susskind, “The anthropic landscape of string theory,” (2003), arXiv:hep-th/0302219.
 - [2] S. R. Coleman and F. De Luccia, “Gravitational Effects On And Of Vacuum Decay,” Phys. Rev. D **21**, 3305 (1980).
 - [3] A. Vilenkin, “The Birth Of Inflationary Universes,” Phys. Rev. D **27** (1983) 2848.
 - [4] A. D. Linde, “Eternally Existing Selfreproducing Chaotic Inflationary Universe,” Phys. Lett. B **175**, 395 (1986).
 - [5] A. D. Linde and M. I. Zelnikov, “Inflationary universe with fluctuating dimension,” Phys. Lett. B **215**, 59 (1988).
 - [6] S. B. Giddings and R. C. Myers, “Spontaneous decompactification,” Phys. Rev. D **70**, 046005 (2004).
 - [7] J. J. Blanco-Pillado, D. Schwartz-Perlov and A. Vilenkin, “Quantum Tunneling in Flux Compactifications,” JCAP **0912**, 006 (2009) [arXiv:0904.3106 [hep-th]].
 - [8] S. M. Carroll, M. C. Johnson and L. Randall, “Dynamical compactification from de Sitter space,” JHEP **0911**, 094 (2009) [arXiv:0904.3115 [hep-th]].
 - [9] P. G. O. Freund and M. A. Rubin, “Dynamics Of Dimensional Reduction,” Phys. Lett. B **97**, 233 (1980).
 - [10] S. Randjbar-Daemi, A. Salam and J. A. Strathdee, “Spontaneous Compactification In Six-Dimensional Einstein-Maxwell Theory,” Nucl. Phys. B **214**, 491 (1983).
 - [11] M. R. Douglas and S. Kachru, “Flux compactification,” Rev. Mod. Phys. **79**, 733 (2007).
 - [12] R. Bousso, O. DeWolfe and R. C. Myers, “Unbounded entropy in spacetimes with positive cosmological constant,” Found. Phys. **33**, 297 (2003) [arXiv:hep-th/0205080].
 - [13] C. Krishnan, S. Paban and M. Zanic, “Evolution of gravitationally unstable de Sitter compactifications,” JHEP **0505**, 045 (2005) [arXiv:hep-th/0503025].
 - [14] G. W. Gibbons, G. T. Horowitz and P. K. Townsend, “Higher Dimensional Resolution Of Dilatonic Black Hole Singularities,” Class. Quant. Grav. **12** (1995) 297.
 - [15] R. Gregory, “Cosmic p-Branes,” Nucl. Phys. B **467**, 159 (1996).

- [16] F. R. Tangherlini, “Schwarzschild field in n dimensions and the dimensionality of space problem,” *Nuovo Cim.* **27**, 636 (1963).
- [17] F. Mellor and I. Moss, “Black Holes And Quantum Wormholes,” *Phys. Lett. B* **222**, 361 (1989); F. Mellor and I. Moss, “Black Holes and Gravitational Instantons,” *Class. Quant. Grav.* **6**, 1379 (1989).
- [18] L. J. Romans, “Supersymmetric, cold and lukewarm black holes in cosmological Einstein-Maxwell theory,” *Nucl. Phys. B* **383**, 395 (1992).
- [19] R. B. Mann and S. F. Ross, “Cosmological production of charged black hole pairs,” *Phys. Rev. D* **52**, 2254 (1995).
- [20] O. J. C. Dias and J. P. S. Lemos, “Pair creation of higher dimensional black holes on a de Sitter background,” *Phys. Rev. D* **70**, 124023 (2004); See also hep-th/0410279 v3.
- [21] R. C. Myers and M. J. Perry, “Black Holes In Higher Dimensional Space-Times,” *Annals Phys.* **172**, 304 (1986).
- [22] R. Basu, A. H. Guth and A. Vilenkin, “Quantum creation of topological defects during inflation,” *Phys. Rev. D* **44**, 340 (1991); R. Basu and A. Vilenkin, “Nucleation of thick topological defects during inflation,” *Phys. Rev. D* **46** (1992) 2345.
- [23] M. Parikh, “Enhanced instability of de Sitter space in Einstein-Gauss-Bonnet gravity,” arXiv:hep-th/0909.3307.
- [24] R. Bousso and S. W. Hawking, “Pair creation of black holes during inflation,” *Phys. Rev. D* **54**, 6312 (1996).
- [25] R. Bousso, “Quantum global structure of de Sitter space,” *Phys. Rev. D* **60**, 063503 (1999).
- [26] J. X. Lu, “ADM masses for black strings and p-branes,” *Phys. Lett. B* **313**, 29 (1993).
- [27] S. W. Hawking and I. G. Moss, “Supercooled Phase Transitions In The Very Early Universe,” *Phys. Lett. B* **110**, 35 (1982).
- [28] J. J. Blanco-Pillado and M. P. Salem, “Observable effects of anisotropic bubble nucleation,” arXiv:1003.0663 [hep-th].
- [29] A. D. Linde, “The Self-Reproducing inflationary universe,” *Scientific American* **271**, 32 (1994).